Arch. Bas. App. Med. 8 (2020): 137 – 145
www.archivesbamui.com
www.ojshostng.com/index.php/abam

Research Article

Histological and Immunohistochemical Study of Pineal and Pituitary Glands of the Greater Cane Rat (*Thryonomys swinderianus*, Temminck 1827)

Gilbert T. T.[1], Olopade F. E.[2*], Mustapha O. A.[3], Folarin O. R.[4] and Olopade J. O[1].
[1]*Department of Veterinary Anatomy, Faculty of Veterinary Medicine, University of Ibadan, Ibadan, Nigeria*
[2]*Department of Anatomy, Faculty of Basic Medical Sciences, University of Ibadan, Ibadan, Nigeria*
[3]*Department of Veterinary Anatomy, College of Veterinary Medicine, Federal University of Abeokuta, Nigeria*
[4]*Department of Biomedical Laboratory Science, College of Medicine, University of Ibadan. Ibadan, Nigeria.*

Received: March, 2020; Accepted: September, 2020

Abstract
The Greater cane rat (GCR) has been proposed as an adaptable native research model due to its unique neurobehavioural attributes, thus the need to establish baseline information on its nervous system. This work was designed to elucidate the cellular architecture and histology of its pineal and pituitary glands. Four pubertal male GCRs were used for this study. Their brains were harvested, and the pineal and pituitary glands carefully dissected. Tissue sections were prepared and stained using haematoxylin and eosin (H&E), Cresyl violet, glial fibrillary acidic protein (GFAP), ionized calcium-binding adapter molecule 1 (IBA1), neuronal nuclei (NeuN) and collagen type 1 antibodies for histological and immunohistochemical analyses. Grossly, the pineal gland of GCR is a pine-cone shaped midline structure and H&E staining showed type I (light) and type II (dark) pinealocytes. Immunohistochemically, astrocytic-like (GFAP+); microglial cells (IBA1+); neurons (NeuN+) and collagen type-1 fibres were localized within the pineal gland. The GCR pituitary gland is a disc-shaped organ located within the sella turcica. Routine staining delineated the neurohypophysis, intermediate lobe and adenohypophysis; fibrous and protoplasmic pituicytes were observed among non-myelinated fibres and Herring bodies in the neurohypophysis. Acidophils, basophils and chromophobes in adenohypophysis, and the melanotrophs in the intermediate lobe were seen. Immunohistochemical studies highlighted GFAP+ pituicytes and collagen type 1 fibres in the neurohypophysis. In conclusion, the histological and immunohistochemical features of pineal and pituitary glands of the GCR are similar to other rodents and mammals, though some peculiarities exist.

Key Words: *Histology, Immunohistochemistry, Pineal gland, Pituitary gland, Greater cane rat.*

INTRODUCTION

The greater cane rat (GCR) *Thryonomys swinderianus* (Temminck, 1827) belongs to the family *Thryonomidae* popularly called grasscutter (Gheban *et al.,* 2019). They are strict herbivorous, mostly nocturnal, although after a certain period of adaptation to their enclosure during captivity, GCR tend to start feeding by day (Aluko *et al.,* 2015). The GCR is indigenous to Africa, and with an average weight of 4kg, it is ranked the second largest rodent in Africa. Because of its large size and delectable flesh, they are hunted by humans in many parts of their geographic range (Mustapha *et al.,* 2020). Distribution is determined by availability of adequate and preferred grass species for food, thus, GCRs are found in virtually all countries of west, east and southern Africa and feed primarily on coarse grasses, however, they also feed on crops in agricultural areas (Kingdon *et al.,* 2013).

The GCR has a relatively long gestation period of 150 days, giving birth to precocial pups. Compared to the laboratory rat with lissencephalic brains, some degree of gyrencephalization have been reported in the GCR – a feature known to influence species' cognitive abilities and sensorimotor skills (Sun and Hevner, 2014). Recently, there has been increased effort to develop home-grown research models, with the GCR being proposed as one of such models, particularly as ecological sentinels for neurotoxicological studies (Mustapha *et al.,* 2019a).

Studies on some aspects of the GCR brain have been reported in literature. Morphological investigations on the GCR brain showed that its mean brain weight approximately

**Author for Correspondence:* Tel: +2348052274102 E-mail: *funmiolopade@yahoo.com*

five times that of the laboratory rat. Dwarika *et al.,* (2008) noted that despite the great difference in brain size and its gyrification, the putative catecholaminergic and serotonergic nuclei in the GCR brain are homologous to those observed in the laboratory rat. Interestingly, the relative brain weight of the GCR is reported to be higher when compared to the gyrencephalic sheep brain which share a similar gestation length. A study of their visual and auditory centres pointed to a greater inclination of the GCR towards auditory-dependent adaptation than to visual acuity (Ibe *et al,* 2017; Ibe *et al.,* 2019). Other investigations on the GCR nervous system reported include: studies on the cerebellum (Obadiah and Obadiah, 2014; Ibe *et al.,* 2016) and also on the macro- and micro-morphometrics and spinal tracings of spinal cord (Mustapha *et al.,* 2015; Mustapha *et al.,* 2017). There is however a dearth of information on pineal and pituitary glands of this rodent.

The pineal gland and the pituitary gland are two important endocrine structures found within the central nervous system (CNS) in the skull (Kaufman *et al.,* 2010). The pineal gland (epiphysis) is a photo-neuroendocrine organ forming part of the epithalamus; it secretes serotonin, melatonin and N,N-dimethyltriptamine (Stehle *et al.,* 2011) and vascularized by the posterior choroidal arteries and the internal cerebral veins (Al-Hussain, 2006). It helps maintain the circadian rhythm, thus further connecting the outside world with internal biochemical and physiological needs and functions of the body (Gheban *et al.,* 2019). The pituitary gland (hypophysis) is a neuroendocrine gland which regulates the body homeostasis during development, stress and other physiological processes. It is an intermediary organ for physiological signal exchanges between the hypothalamus and the peripheral organs. This small organ is usually localized in a tiny bony cavity called *sella turcica*, covered by a dural fold named *diaphragm sellae* (Perez-Castro *et al.,* 2012). This work was designed to investigate the histological and cellular architecture of these two endocrines (pineal and pituitary) glands of the GCR in order to better understanding the biology of this unique African rodent.

MATERIALS AND METHODS

Animals: Four pubertal male GCR, 7-8 months old with a mean body weight of 2.13± 0.09kg were obtained from a commercial farm, Pavemgo® Grasscutter in Badagry, Lagos State, Nigeria, reputable for keeping birth records of GCR reared in captivity. They were transported in metallic cages with adequate ventilation and acclimatized for 48 hours prior to sacrifice at the animal house of the Neuroscience Unit, Department of Veterinary Anatomy, University of Ibadan, Nigeria. Food and water were provided *ad libitum*. At the time of sacrifice, the body weight of each rodent was obtained with a digital electronic balance (Zhongshan Camry Electronic Co. Ltd, China).

Experimental procedure: The rodents were sacrificed based on the protocol of Olopade *et al* (2011). They were deeply anesthetized (ketamine 100 mg/kg body weight and xylazine 10 mg/kg body weight, intraperitoneal) and perfused transcardially with normal saline followed by 10% neutral buffered formalin (NBF). The brains were subsequently harvested from the skull and, the pineal and pituitary glands were carefully dissected.

Histology: This was followed by post-fixation in 10% NBF at 4°C for 48 hours. Haematoxylin and Eosin, and Cresyl violet staining of the pineal and pituitary glands were carried out following the methods described by Olopade *et al.,* (2011) and Mustapha *et al.,* (2019b). Prepared slides were viewed using the MYCH-101 microscope (Inspiration Marvotech®, Belgium) equipped with a CEFC Industrial digital camera.

Immunohistochemistry: The pineal and pituitary brain tissues were prepared for immunohistochemistry following the protocol described by Usende *et al.,* (2016). Briefly, 5µm thick paraffinized brain sections were mounted on adhesive glass slides, well labeled with pencil and baked in an oven set at 60°C for 1 hour 30 minutes to melt the wax. Deparaffinization of the sections was done in 2 changes of xylene, after which the sections were hydrated in decreasing concentration of alcohol to water. Sections were then rinsed in double distilled water before retrieval of antigen was achieved by incubating the sections in 10 mM citrate buffer at pH of 6.0 for 25 minutes to unmask the hidden antigenic site. In order to reduce non-specific antibody binding and to hinder endogenous peroxidase activities, sections were treated with 30% H_2O_2/methanol. Sections were subsequently blocked by incubating in 2% PBS milk while on a rocker for 60 minutes. Consecutive sections were immune-labeled with the following antibodies: rabbit anti-IBA 1 antibody (dilution 1:1000, Wako Pure Chemical Industries Ltd., Japan) for microglial cells, rabbit anti-glial fibrillary acidic protein (GFAP) (1: 1000; Dako, Denmark), to visualize astrocytes; rabbit anti-NeuN polyclonal antibody (dilution 1:500, EMD Millipore, USA) to visualize neurons and rabbit polyclonal anti-collagen type 1 (1:200, Abcam Inc, USA), for Type 1 collagen. The antibodies were diluted in 1% PBS milk and 0.1% Triton X detergent (to facilitate quick penetration of antibody) and the samples underwent incubation overnight at 4°C. HRP-conjugated secondary antibodies were subsequently used following manufacturer's protocol (dilution 1:200, Abcam Inc, USA) to detect the bound antibody. The end product of entire reaction was improved with 3, 3'-diaminobenzidine a chromogen (1:25 dilution, Victor Laboratories, USA) for 5 minutes. Subsequently, sections were dehydrated in solutions of graded alcohol concentrations, and alcohol removed by passing through two changes of xylene (5 minutes each), then mounted wet in permount (toluene based mountant, Atom Scientific, Manchester), cover slipped and allowed to dry. Microscopic examination was carried out using MYCH-101 microscope (Inspiration Marvotech, Belgium).

RESULTS

Gross Examination: The cerebrum was separated from the cerebellum to expose the epithalamus. The pineal gland was found "hidden" between cerebrum and cerebellum. When they were separated craniocaudally, the pineal gland is seen as an unpaired midline rounded elevation. The pineal gland of GCR was pinecone shaped located rostromedial to the rostral colliculi, with the bilaterally paired *habenulae* which continue rostrally and laterally to the pineal recess. The gland was situated in the midline between the two cerebral hemispheres,

caudodorsal to the third ventricle and in front of the rostral colliculi (Plate 1).

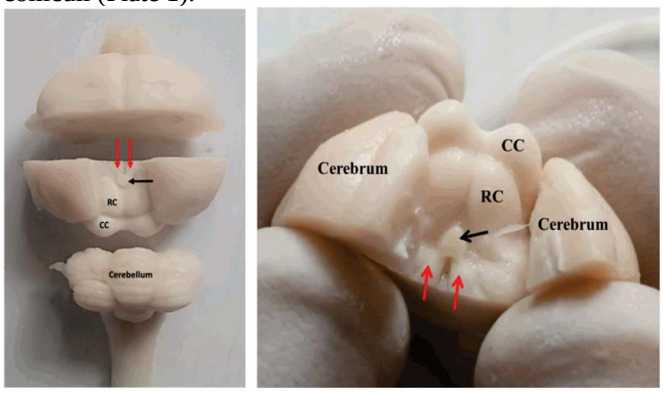

Plate 1:
Photographs of GCR brain showing the pineal gland (black arrows) and the bilaterally located *habenulae* (red arrows). RC, rostral colliculus; CC, caudal colliculus.

The pituitary gland was located in the sella turcica (Fig. 2A) which appeared as a shallow depression on the sphenoid bone (Fig. 2B). The pituitary gland is hidden in the sella turcica of the sphenoid bone from which it was extracted. The pituitary gland was disc-shaped (Fig. 2C) and was enclosed by a common capsule. The capsule was tightly attached to it except at the upper part, the area of connection of the pituitary gland with the infundibulum. The anterior pituitary (adenohypophysis) and posterior pituitary (neurohypophysis) lobes were distinguishable on gross examination. The pituitary gland was connected to the hypothalamus through the infundibular stalk (Fig. 2D).

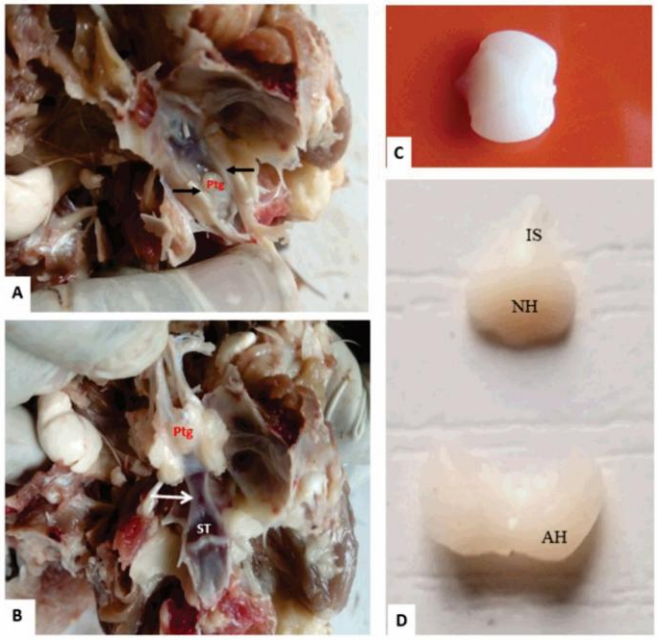

Plate 2:
Photographs of the GCR pituitary gland. **A**. The pituitary gland still lying in the *sella turcica* of the sphenoid bone. The trigeminal nerves (black arrows) are seen on the lateral sides of the pituitary gland (Ptg); **B**. Location of the pituitary gland (Ptg) in the *sella turcica* (ST). The *sella turcica* here appeared as a shallow depression in the caudal part of the sphenoid bone (white arrow); **C**. Dorsal view of the pituitary gland (Ptg) showing its disc-shaped; **D**. The pituitary gland showing the neurohypophysis (NH) separated from the adenohypophysis (AH) with some part of infundibular stalk (IS).

Histological findings: The GCR pineal gland (Plate 3A, 4A and 5A) was surrounded by thick fibrous connective tissue capsule made of pia mater, one layer of meninges (Fig. 3B, 4B and 5B). The pinealocytes and glial cells are the two types of parenchymal cells. The number of pinealocytes observed exceeded the number of glial cells, and they were present singly or in form of irregular cords or clusters. These pinealocytes were oval to round in shape and are the major parenchymal cells found in the pineal gland with lightly basophilic cytoplasm and euchromatic nuclei. The pinealocytes are divided into light pinealocytes or type I pinealocytes which stained at low density when viewed under light microscope (Fig 3B), and dark pinealocytes or type II pinealocytes which stained at high density and are less in numbers when compared to light pinealocytes (Fig 3C and 4C). Cresyl violet stain showed cells with elongated strong basophilic nuclei. These cells had extensions which stretched out between the pinealocytes, this is compatible to astrocytes (Fig. 4C). The GCR pineal gland had pineal lobules which were located at dorsal part of the gland with pinealocytes found around the lobules (Plate 5A).

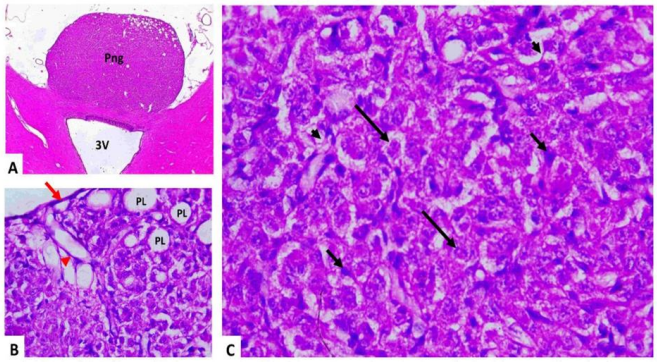

Plate 3:
Photomicrographs of the GCR pineal gland. A. The entire coronal section of pineal gland (Png) seen above the third ventricle (3V) (H&E, x40); B. The parenchyma of the gland showing; pial capsule (red arrow), pineal follicles (PL) and cytoplasmic processes (red arrow head) of pinealocytes (H&E, x400); C. The dark pinealocytes (long black arrows) and light pinealocytes (short black arrows) are also seen in the parenchyma of the gland. Cytoplasmic process of pinealocytes (arrow head) (H&E, x400).

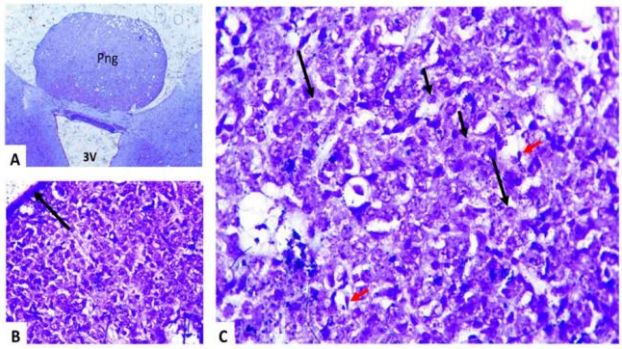

Figure 4:
Photomicrographs of the GCR pineal gland. A. The entire coronal section of the pineal gland (Png) seen above the third ventricle (3V) (Cresyl, x40); B. The capsule (long black arrow) seen covering the dorsal part of the gland (Cresyl, x400); C. The gland showing type I (light) pinealocytes (long black arrow) and type II (dark) pinealocytes (short black arrow). Nerves fibers and astrocytes (red arrow) are seen separating the pinealocytes in the parenchyma (Cresyl, x400).

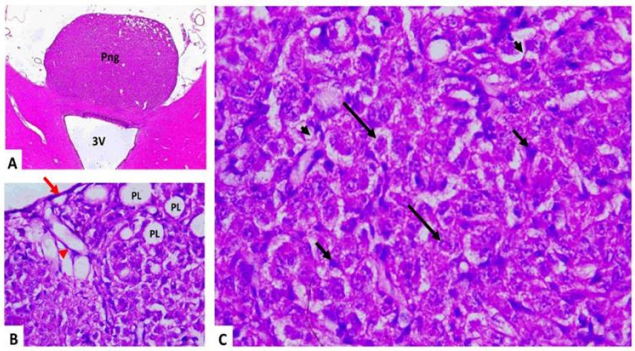

Figure 5:
Photomicrographs of the GCR pineal gland. A. The location of pineal lobules at the dorsal part of the gland. (H&E, x40); B. Section of the gland showing its dorsal part where the pineal lobules are located. The pial capsule (black arrow) is found round the dorsal part. (H&E, x100); C. Higher magnification of the pineal gland showing the pineal lobules (PL). The lobules with tubular aspect include the pinealocytes (red arrow) around them. (H&E, x400).

The pituitary gland of the GCR was covered by pial capsule (Fig. 6B). It consists of the adenohypophysis (anterior lobe) and neurohypophysis (posterior lobe), separated by the hypophyseal cleft (Fig. 6B). The melanotrophic cells of intermediate lobe of GCR (Fig. 6C and 9C) are well developed and were easily distinguished. Based on staining properties, the cells of the adenohypophysis were divided into three main types: chromophilic acidophils, chromophilic basophils and chromophobes. The adenohyphopysis cells are arranged in clusters and cords (Fig. 8 and 9F). The neurohypophysis of GCR is largely made of nerve fibers, with 2 types of supportive astrocytic glial cells/pituicytes: fibrous pituicytes which have round nuclei and protoplasmic pituicytes with elongated nuclei. The herring bodies being the neurosecretory bodies and non-myelinated nerve fibres are found among the pituicytes in the neurohypophysis. Three types of pituicyte nuclei were identified in the GCR neurohypophysis: oval shaped nucleus, triangular shaped nucleus and elongated shaped nucleus (Fig. 6).

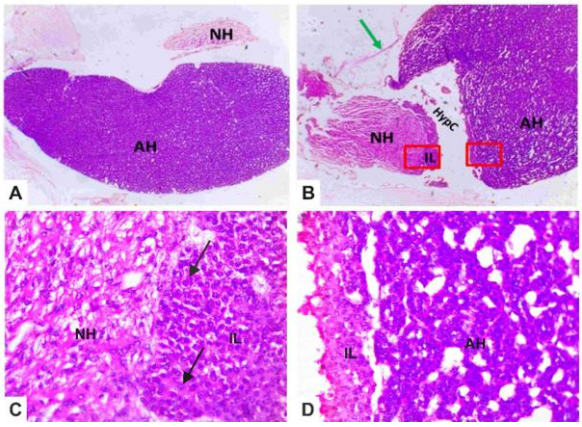

Figure 6:
The photomicrographs of pituitary gland of the GCR. A. The gland showing the adenohypophysis (AH) and neurohypophysis (NH) (H&E, x40); B. The gland showing the intermediate lobe (IL) located between the adenohypophysis (AH) and neurohypophysis (NH). The hypophyseal cleft (HypC) is also seen. Green arrow is showing the capsule (H&E, x40); C. A higher magnification of the neurohyphophysis (NH) and the melanotrophic cells (black arrow) of intermediate lobe (IL) (H&E, x400); D. The gland showing a higher magnification of the adenohyphophysis (AH) and intermediate lobe (IL) (H&E x400).

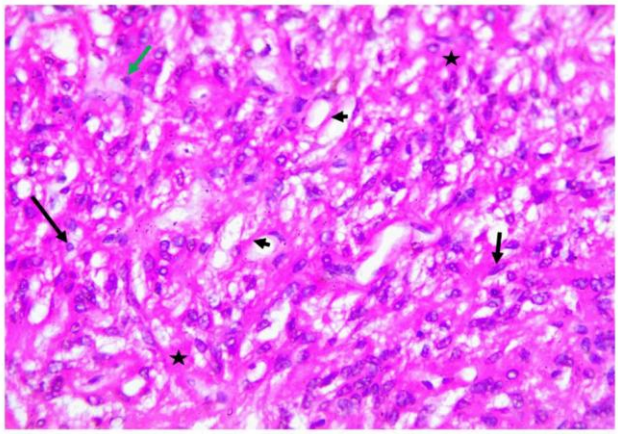

Figure 7:
The neurohyphopysis of GCR pituitary gland showing the fibrous pituicyte (long black arrow), protoplasmic pituicyte (short black arrow), herring bodies (black stars) and non-myelinated nerve fibres (black arrow heads). Three types of pituicyte nuclei were identified in the neurohypophysis: oval shaped nucleus (long black arrow), triangular shaped nucleus (green arrow) and elongated shaped nuclei (short black arrow) (H&E, x400).

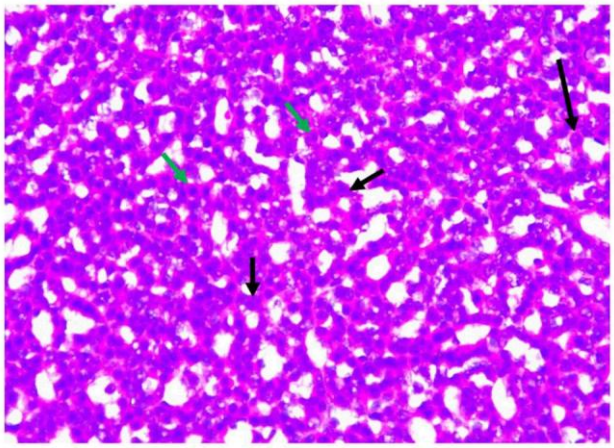

Figure 8:
The adenohyphopysis of GCR pituitary gland showing the chromophilic basophils (green arrow) with lightly stained cytoplasm; chromophilicacidophils (short black arrow) which is stained with eosin and chromophobes (long black arrow) which are the largest cells in adenohypophysis. The adenohyphopysis cells are arranged in clusters and cord of cells (H&E, x400).

Immunohistochemical Examination

Glial fibrillary acidic protein (GFAP): GFAP was used for immunoreactive expression of astrocytic-like cells of the GCR pineal gland and pituicytes of the neurohypophysis (posterior lobe) of the pituitary gland. The pineal gland of GCR displayed immunoreactive expression of GFAP by the astrocytic-like cells (interstitial cells). The long and slender processes of the interstitial cells or astrocytic-like cells are distinct in the pineal gland of GCR (Fig. 10B).

The GCR pituitary gland revealed the expression of GFAP-positive pituicytes. The pituicytes are resident astrocytes of the neurohypophysis found between the non-myelinated fibres from the paraventricular and supraoptic neurons of hypothalamus. The pia mater around the gland shows immunopositive reaction to GFAP, suggesting the presence of subpial astrocytes (Fig. 11B). The adenohypophysis of GCR showed no immunoreactivity to GFAP (Fig. 11F).

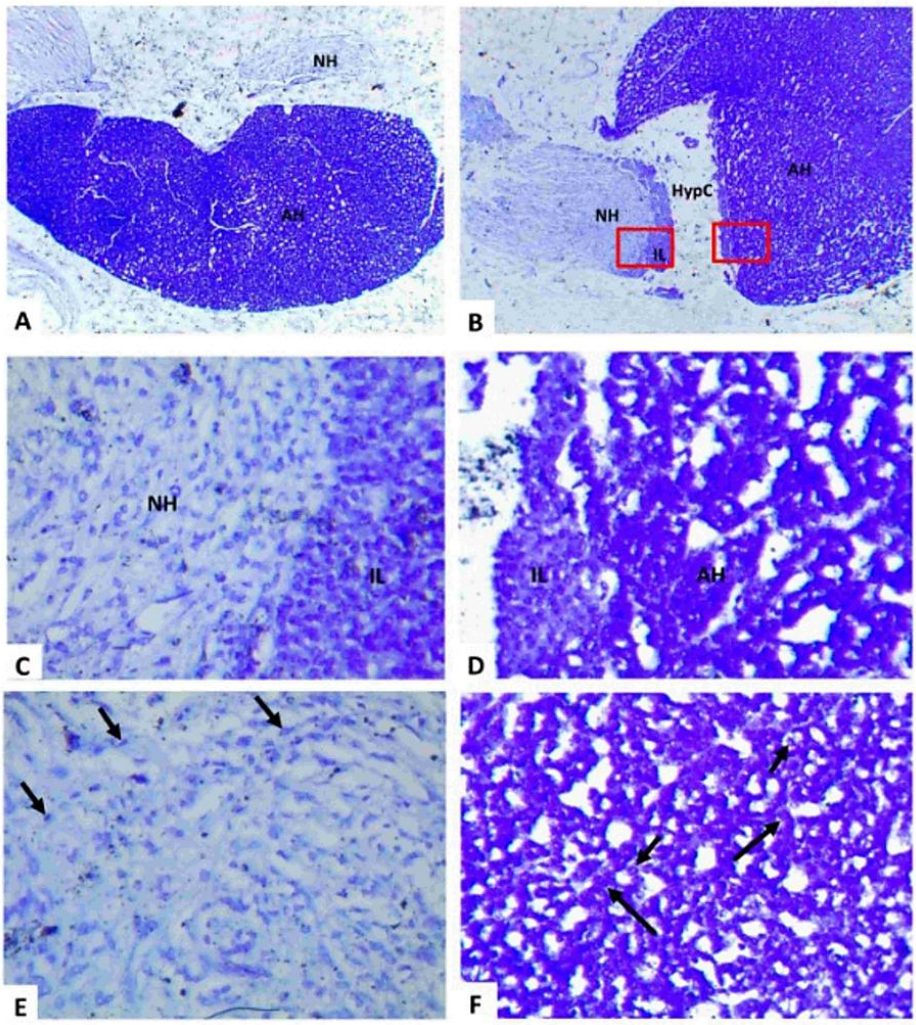

Figure 9:
Photomicrograph of the GCR pituitary gland. A. The pituitary gland showing the adenohypophysis (AH) and neurohypophysis (NH) (Cresyl x40); B. The gland showing the intermediate lobe (IL) and hypophyseal cleft (HypC) are located between the adenohypophysis (AH) and neurohypophysis (NH) (Cresyl x40);C.The gland showing a higher magnification of the neurohypophysis (NH) and intermediate lobe (IL) (Cresyl, x400); D. The gland showing a higher magnification of the adenohypophysis (AH) and intermediate lobe (IL) (Cresyl, x400); E. The gland showing nuclei (black arrow) of pituicytes in the neurohypophysis (Cresyl x400); F. The gland showing the chromophils (small black arrow) and chromophobes (long black arrows) of the adenohypophysis (Cresyl x400).

IBA1: IBA1 was used to highlight the presence of microglia or phagocytic cells in the pineal and pituitary glands. The pineal gland of GCR showed the expression of the perivascular microglia round the blood vessel and capsular microglia were also seen in the pial capsule of the pineal gland (Fig. 12). The adenohypophysis and neurohypophysis of the pituitary gland of GCR showed no immuoreactivity to IBA1. The pia mater that surrounds the pituitary gland was immunoreactive to IBA1 because they have microglia (meningeal microglia) (Fig. 13).

NeuN: The pinealocytes in the GCR pineal gland had no immunoreactivity to NeuN antibody. However, there was immunopositive reaction shown by the few neurons in the gland (Fig. 14). The adenohypophysis and neurohypophysis of pituitary gland of the GCR displayed immunonegative reaction to NeuN.

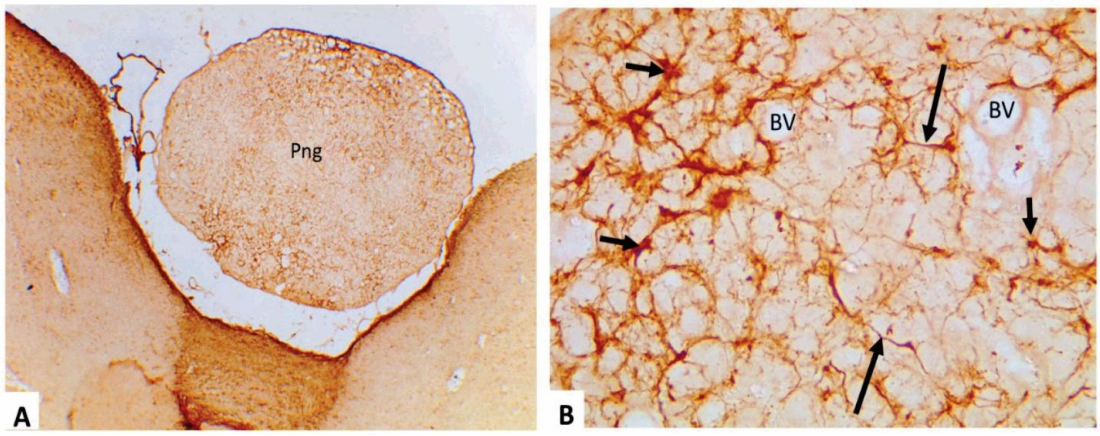

Figure 10:
Photomicrographs of coronal section of the pineal gland of GCR showing immunoreactivity of GFAP. **A.** The pineal gland showing the entire coronal section of the pineal gland (Png) (GFAP x40). **B**. The parenchyma of the gland showing Interstitial cells or astrocytic-like cells (short black arrow) with their slender and long processes (long black arrow) and blood vessel (BV) within the parenchyma of the gland (GFAP, x400).

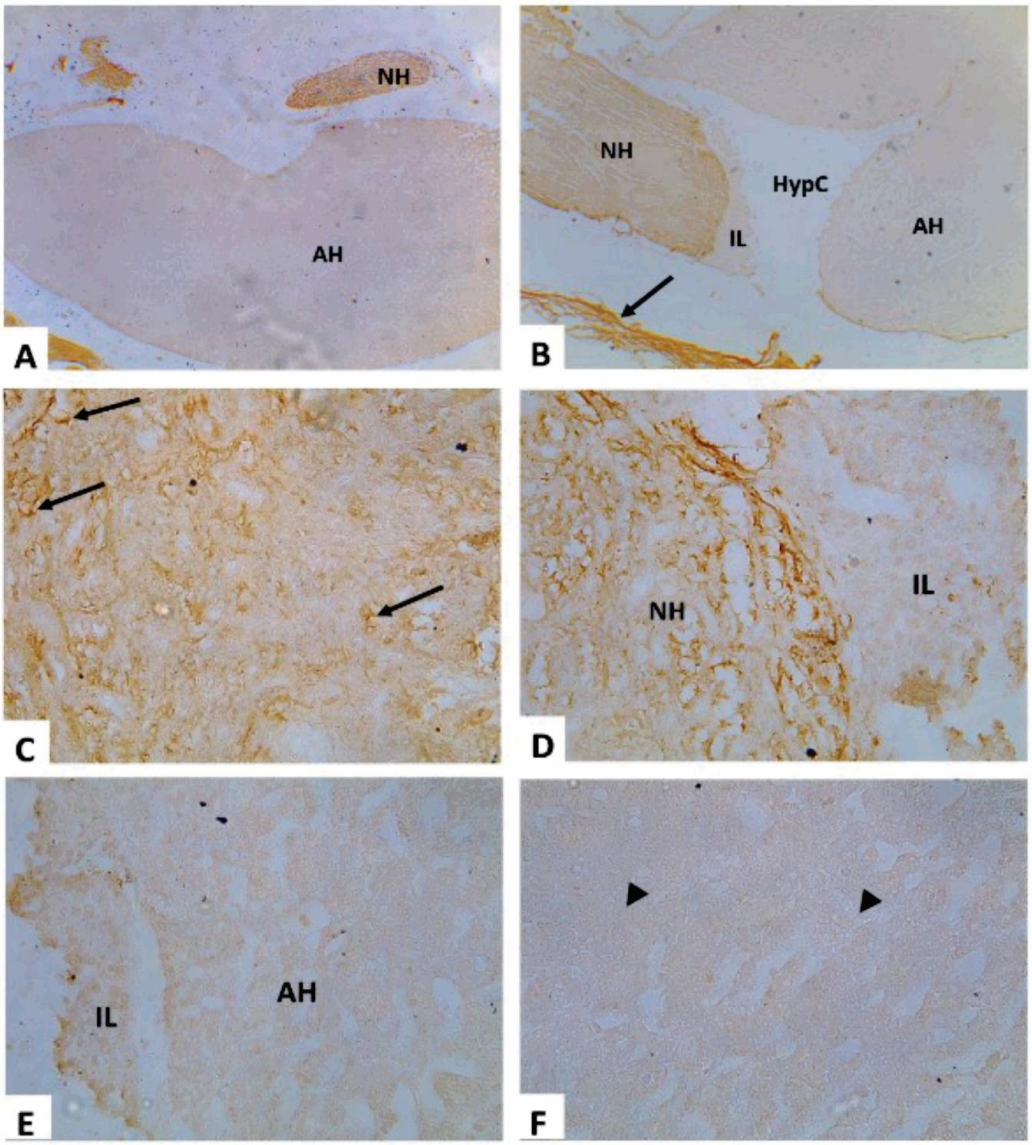

Figure 11:
Photomicrographs of GCR Pituitary gland showing immunoreactivity to GFAP. **A.** The gland showing the adenohypophysis (AH) and neurohypophysis (NH) (GFAP, x40); **B**. The gland showing adenohypophysis (AH), intermediate lobe (IL), neurohypophysis (NH) and the hypophyseal cleft (HypC). The adenohypophysis and intermediate lobe show negative immunoreactions. The pia mater (black arrow) around the gland shows immunopositive reaction to GFAP (GFAP x40); **C.** The gland showing the expression of pituicytes (black arrows), which are resident astrocytes of the neurohypophysis. (GFAP, x400). **D-F**. The gland showing the neurohypophysis (NH), adenohypophysis (AH), intermediate lobe (IL), pituicytes (black arrow) in the neurohypophysis. The chromophils and chromophobes of adenohypophyis are GFAP immunonegative. (**D-F:** GFAP, x400).

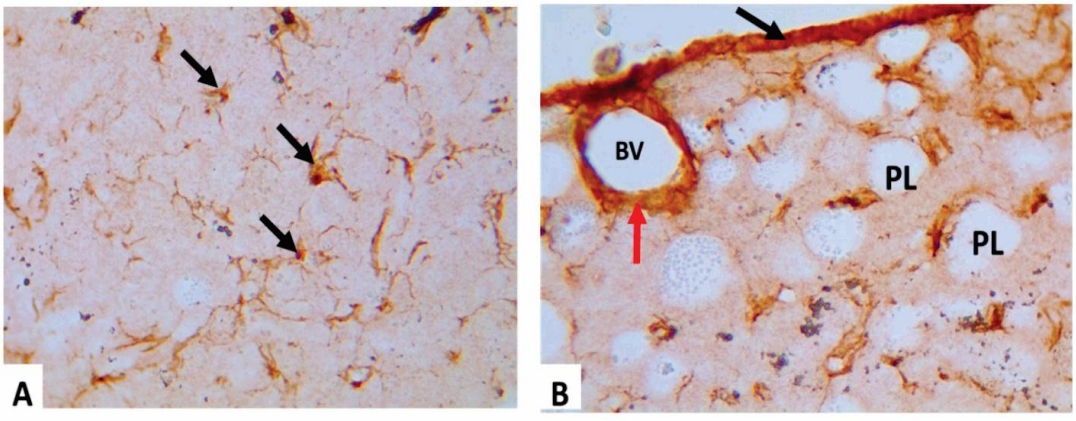

Figure 12:
Photomicrographs of the GCR pineal gland: A. The parenchyma of the pineal gland showing the expression of microglia (long black arrow). (IBA1, x400). B. The pineal gland showing the expression of the perivascular microglia (red arrow) round the blood vessel (BV) and capsular microglia (short black arrow); PL. pineal lobule (IBA1, x400).

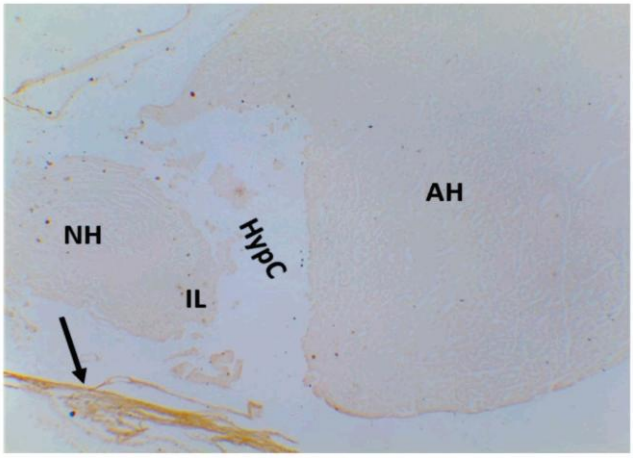

Figure 13:
Photomicrograph of the GCR pituitary gland shows that the pituitary gland is immunonegative to IBA1. The pia mater (black arrow) around the pituitary gland is immunopositive to IBA1 (IBA1, x400).

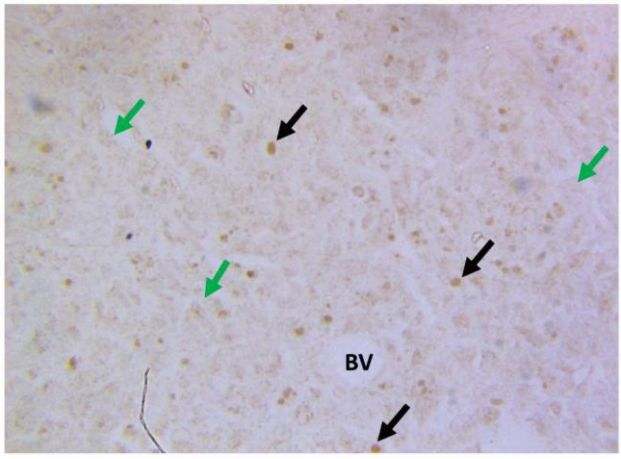

Figure 14:
Photomicrograph of the GCR pineal gland showing expression of the few neurons (black arrows) present in the gland. The numerous pinealocytes (green arrows) in the gland are immunonegative to NeuN. BV, blood vessel (NeuN, x400).

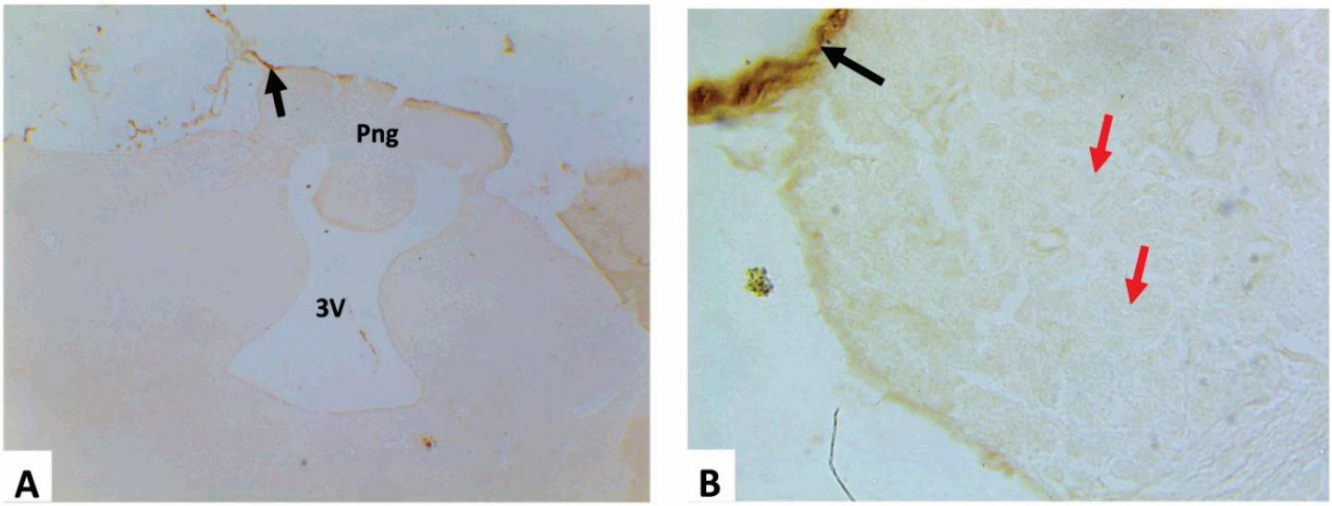

Figure 15:
Photomicrographs of pineal gland of the GCR. **A.** The pineal gland (Png) showing the capsule which is immunopositive for collagen type 1 antibody. (Collagen1, x40); **B.** Higher magnification of the gland showing the expression of collagen type 1 fibers is capsule of the gland. The pinealocytes (red arrow) are immunonegative to collagen type 1 (Collagen1, x400).

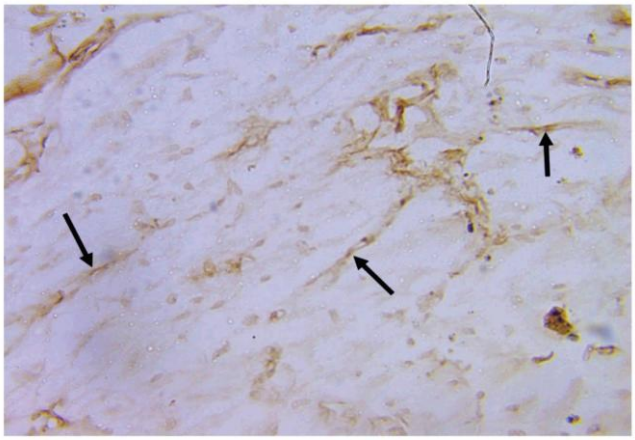

Figure 16:
Photomicrograph of GCR pituitary gland showing collagen fibers which are present between unmyelinated nerves fibers and pituicytes in the neurohypophysis (Collagen1, x400).

Collagen type 1 (Collagen1): The pineal gland of the GCR showed the expression of collagen type 1 fibres in the gland (Fig. 15B). The pituitary gland of the GCR showed the expression of collagen present between unmyelinated nerves fibers and pituicytes in the neurohypophysis. (Fig. 16).

DISCUSSION

The location of the pineal gland of African greater cane rat (GCR) in this study was similar to that described in other mammals including rats, donkey, rabbit (Hendelman, 2000; Dyce *et al.*, 2002, Frandson *et al.*, 2009, Ebada, 2012; Nawal *et al.*, 2012, Busolini *et al.*, 2017, Soliman *et al.*, 2019). In spite of common origin of pineal gland in mammals (Vollrath, 1981), the gland has different shapes in rodents; oval-round shape in hamster (Gregorek *et al.*, 1977), elongated and dumb bell shaped organ in guinea pig (Vollrath, 1981), round-shaped in degu, a rat-like South American rodent (Uria *et al.*, 1992), tonsilar-like shape in mice (Matsunaga *et al.*, 2017), oval shape in viscacha, a South American rodent (Busolini *et al.*, 2017) and fusiform-like mass in rabbit (Soliman *et al.*, 2019). The pineal gland in GCR is pine-cone shaped, white in colour and not pigmented as compared to the bat (Bhatnagar and Hilton, 1994).

The pituitary gland of the GCR was located at the base of the brain, on the sphenoid bone, as described for domestic mammals (Dyce *et al.,* 2010). The gland was in an ill-defined depression of the sphenoid bone called *sella turcica*. Our results corroborate those of Mahmood (2014) who described the anatomical and histological features of the pituitary gland in rats and found that for most investigated species, there was no true *sella turcica*, but rather, a shallow depression in the sphenoid bone. The gland is disc shape as reported in rat (Mahmood 2014). The pituitary gland was also seen between the two roots of trigeminal nerve of GCR as reported by Cao *et al.,* (2017) in mouse.

Histologically, the GCR pineal glands are also covered by a connective tissue capsule arising from the pia-mater as described in mice (Matsunaga *et al.,* 2017). However, meningeal septa in GCR does not project or enter the parenchyma of the gland. This is similar with the findings of Lima *et al.,* (2011) in sheep. In mice, this capsule projects into the parenchyma forming lobular structures (Matsunaga *et al.,* 2017). We described two types of pinealocytes using H&E stain, these are; light (type I) and dark (type II) pinealocytes. These characteristics are similar to those described by Soliman (2019) in rabbits. The Cresyl violet stain showed interstitial, astrocytic-like cells with elongated nuclei as reported in mice by Matsunaga *et al.,* (2017). Brain sand (calcified concretions predominantly composed of calcium and magnesium salts) was not found in any of the studied pineal glands of the GCR. This absence was also reported in dogs (Gomes, 2003). However, it is worthy of note that the analyzed pineal glands are from pubertal (young adult) males. It is possible that further studies may reveal their presence in aged animals.

The neurohypophysis is considerably smaller than the adenohypophysis and blood vessels were not filled with blood, which confirmed previously published data by Mahmood (2014) in rat. In this study we also found that the adenohypophysis and the neurohypophysis were in contact and joined through the intermediate lobe as reported by Mahmood (2014) in rat. The avian do not have intermediate lobe as shown by Jahangirfard *et al.,* (2019) in turkeys and the intermediate lobe is poorly developed in primate as reported by Dyce *et al.,* (2010), while the human pituitary gland lacks the intermediate lobe and hypophyseal cleft (Perez-Castro *et al.,* 2012). The parenchymal cells of the adenohypophysis are divided into three broad types: chromophilic acidophils, chromophilic basophils and chromophobes. These cells in adenohypophysis are arranged as clusters or cords of cells as reported by Mahmood (2014). Using H&E, the neurohyphopysis revealed two types of pituicytes: fibrous and protoplasmic, as described by Ye *et al.,* (2018) in camels. Furthermore, three types of pituicyte nuclei were identified in the GCR neurohypophysis: as oval shape nucleus, triangular shape nucleus and elongated shaped nucleus. These types of pituicyte nuclei shape were described by Mahmood (2014).

REFERENCES

Al-Hussain S. 2006. The pinealocytes of the human pineal gland: a light and electron microscopic study. Via Med. 65(3):181-187.

Aluko, F., A. Salako, L. Ngere and O. Eniolorunda. 2015. A review of the habitat, feeds and feeding, behavior and economic importance of Grasscutter farming. Amer J Res Comm. 3(9):96-107.

Angela, N., A.N. Viaene, E.B. Lee, J.N. Rosenbaum, I.M Nasrallah, and M.P. Nasrallah. 2019. Histologic, immunohistochemical, and molecular features of pituicytomas and atypical pituicytomas. Acta Neuropath Comms. 7:6.

Bhatnager, K.K., and F.K. Hilton. 1994. Observations on the pineal gland of the big brown bat, Eptesicusfuscus: Possible correlation of melatonin intensification with constant darkness. Anat Rec. 240(3).

Busolini, F.I., G.J. Rosales, V.P. Filippa, and F.H. Mohamed. 2017. A seasonal and age-related study of interstitial cells in the pineal gland of male viscacha (Lagostomus maximus maximus). Anat Rec. 300:1846-1857.

Cao, D., X. Ma., W.J. Zhang, and Z. Xie. 2017. Dissection and coronal slice preparation of developing mouse pituitary gland. JOVE. 129:e56356, doi: 10.3791/56356.

Dwarika, S., B.C. Maseko, A.O. Ihunwo, K. Fuxe, and P.R. Manger. 2008. Distribution and morphology of putative catecholaminergic and serotonergic neurons in the brain of the greater cane rat (Thryonomys swinderianus). J. Chem. Neuroanat. 35:108-122.

Dyce. K.M., W.O. Sack, and C.J.G. Wensing. 2002. Textbook of veterinary anatomy, 3rd edition. Saunders. An Imprint of Elsivier Sci, St Louis, Missouri. 860 pp.

Dyce, K.M., W.O. Sack, and C.J.G. Wensing. 2010. Textbook of veterinary anatomy, 4th edition, Saunders. An Imprint of Elsevier Inc, St Louis, Missouri. 268-290.

Ebada, S. 2012. Morphological and Immunohistochemical Studies on the Pineal Gland of the Donkey (Equus asinus). J. Vet. Anat. 5(1):47-74.

Frandson, R.D., W. Lee, and A.D. Fails. 2009. Anatomy and physiology of farm animals, 7th edition. Lea and febiger, Philadelphia. pp:288-302.

Gheban, B.A., I.A. Rosca, and M. Crisan. 2019. The morphological and functional characteristics of the pineal gland. Neurol Med Pharm Rep. 92(3):226 – 234.

Gomes, L.A. 2003. Estudo Morfológico da glândula pineal no cão. Universidade de São Paulo, Sao Paulo. 85 pp.

Gregorek, J.C., H.R. Seibel, and R.J Reiter. 1977. The pineal complex and its relationship to other epithalamic structures. Acta Anat (Basel). 99:425-34.

Hendelman, W.J. 2000. Atlas of functional neuroanatomy. CRC Press, New York. pp:240.

Humbert, W., F. Cuisinier, V.J. Jean-Claude, and P. Pévet. 1997. A possible role of collagen fibrils in the process of calcification observed in the capsule of the pineal gland in aging rats. Cell Tissue Res. 288:435–439.

Ibe, C.S., S.A Ojo, S.O. Salami, J.O., J.O. Ayo, U.C. Nlebedum, and E. Ikpegbu. 2016. Cytoarchitecture and brain-derived neurotrophic factor immunolocalisation in the cerebellar cortex of African grasscutter (Thryonomys Swinderianus). J. Morphol. Sci., 33(3):146-154

Ibe, C.S., E. Ikpegbu, U.C. Nlebedum. 2017. Comparative morphology of the visual and auditory reflex centres in the African grasscutter (Thryonomys swinderianus-Temminck, 1827). Italian J. Anat. Embryol. 122:196-205.

Ibe, C.S., S.O. Salami, E. Ikpegbu, and M. Adam. 2019. Histology and Brain Derived Neurotrophic Factor immunoreaction of the neurons in the corpora quadrigemina of the African grasscutter (Thryonomys swinderianus – Temminck, 1827). Agric Trop Subtrop. 52(2):49-58

Jahangirfard, R., A. Shalizar-Jalali, R. Shahrooz, G. Najafi, and A. Minas. 2019. Anatomical and cytohistological study of the pituitary gland in adult turkey. Vet Res For. 10(2):159 -163.

Kaufman, M., A.Y. Nikitin, and J.P. Sundberg. 2010. Histologic basis of mouse endocrine system development: a comparative analysis. CRC Press, Boca Raton, FL. 245 pp

Kingdon J, Happold D, Hoffmann M, Butynski T, Happold M, Kalina J. 2013. Introductory Chapters and Afrotheria. In Mammals of Africa. Volume III. Bloomsbury Publishing, London. 1-63.

Kus, I., M. Sarsilmaz, O. Aslan, T. Ozdem, H. Pekmez, A. Songur, and H. Kelestimur. 2004. Light and electron microscopic examination of pineal gland in rats exposed to constant light and constant darkness. Neuroendocr Let. 25:102-108.

Lima, E.M.M., M.I.S. Santana, M.B. Castro, H.G. Benedicto, P.M. Ferreiral, and A.R.C.B. Vianna. 2011. Microstructure and morphoquantitative study of pineal gland in Santa Ines sheep ARS VET, Jab, SP. 27(3):186-191.

Mahmood, H.B. 2014. Anatomical and histological study of pituitary gland of the rats in Iraq. J Kerb Uni.12:221-228.

Maślińska, D., M. Laure-Kamionowska, K. Deręgowski, and S Maślińsk. 2010. Association of mast cells with calcification in the human pineal gland. Fol Neuropath. 48(4).

Matsunaga, M.M., F. Crunfli, G.J.M Fernandes, W.C. Rossi Jr, and A. Esteves. 2017. Morphologic analysis of mice's pineal gland. J. Morphol. Sci. 28(3):157-160.

Møller, M., F. Martin, M.F. Rath, and D.C. Klein. 2006. The perivascular phagocyte of the mouse pineal gland: an antigen-presenting cell. Chronobio Int. 23(1&2):393–401.

Mustapha, O.A., O.A. Aderounmu, M.A. Olude, M.E. Okandeji, A.K. Akinloye, B.O. Oke, and J.O. Olopade. Anatomical Studies on the Spinal Cord of the Greater Cane Rat (Thryonomys swinderianus, Temminck) 1: Gross Morphometry. Nig Vet J. 36(2):1192-1202.

Mustapha, O.A., S. Taiwo, A.M. Olude, O.A. Aderounmu, M.E Okandeji, A.K. Akinloye, J.O. Olopade, and B.O. Oke. 2017. Anatomical studies on the spinal cord of the greater cane rat (Thryonomys swinderianus, Temminck) II: Histomorphology and spinal tracings. Nig Vet J. 38(2):129-139.

Mustapha, O.A., M.A. Olude, S. Ezekiel, J. Seeger, S.A. Fietz, and J.O. Olopade. 2019a. Developmental horizons in the pre-natal development of the Greater cane rat (Thryonomys swinderianus). Anat Hist Emb.48(2):231-238.

Mustapha, O.A., M.A. Olude, B. Taiwo, and J.O. Olopade. 2019b. Cytoarchitecture of the hippocampal formation in the African giant rat (Cricetomys gambianus, Waterhouse). Niger J of Phy Sci. 34(1):55-62.

Mustapha, O.A., E.E. Teriba, O.S. Ezekiel, A.M. Olude, A.K. Akinloye, and J.O. Olopade. 2020. A study of scientific publications on the greater cane rat (Thryonomys swinderianus, Temminck 1827). Ani Mod Exp Med. 00:1–9.

Nawal, S.O., H.I. Ismail, and D.I. Osman. 2012. Morphology of the pineal gland of the one humped camel (Camelus dromedarius). U of K. J. Vet. Med. and Anim. Prod. 3(2):65-81.

Nishimura, S., S. Tabata, Y. Nakamura, K Okano, and H. Iwamoto. 2004. Three-Dimensional Architecture and Distribution of Collagen Components in the Goat Hypophysis. Anat Rec 277A:275–286.

Obadiah, B., and H.I. Obadiah. 2014. Cytoarchitectural study of the cerebellum of greater cane rat (Thryonomys swinderianus). J Res An Sci. 2(2):105-116.

Olopade, J.O., I.O. Fatola, and F.E. Olopade. 2011. Vertical Administration of vanadium through lactation induces behavioural and neuromorphological changes: protective role of vitamin E. Niger J Phy Sci. 26(1):55-60.

Perez-Castro, C., U. Renner, M.R Haedo, G.K. Stalla, and E. Arzt. 2012. Celllular and molecular specificity of pituitary gland physiology. Physiol Rev. 92:1-38.

Redondo, E., A. Franco, A.J. Masot, and S. Regodon. 2001. Ultrastructural and immunocytochemical characterization of interstitial cells in pre- and postnatal developing sheep pineal gland. Eur J Histochem. 45:249–258.

Soliman, S.M.M., K.M. Mazher, T.M. Nabil, U.K. Moawad, and R.M. Hassan. 2019. Histochemical, immunohistochemical and ultrastructural identification and characterization of neurosecretory cells of pineal gland. Asian J Biol Sci.12: 702-710.

Stehle, J.H., A. Saade, O. Rawashdeh, K. Ackermann, A. Jilg, and T. Sebestény. A survey of molecular details in the human pineal gland in the light of phylogeny, structure, function and chronobiological diseases. J Pineal Res. 51:17–43.

Sun, T., and R.F. Hevner. 2014. Growth and folding of the mammalian cerebral cortex: from molecules to malformations. Nat Rev Neurosci. 15(4):217-232. doi:10.1038/nrn3707

Temminck CI. 1827. Thryonomys swinderianus, (Temmninck, 1827). Monographies de Mammal I. Sierra Leone. 248.

Uria, H., I. Antolin, D. Tolivia, M.J. Rodriguez-Colunga, and A. Menendez-Pelaez. 1992. The pineal gland of the trumpet-tailed rat (Octodon degus). J Pineal Res. 13:174-83.

Usende, I.L., D.F Leitner, E. Neely, J.R. Connor, and J.O. Olopade. 2016.The deterioration seen in myelin related morphophysiology in vanadium exposed rats is partially protected by concurrent iron deficiency. Niger J Phy Sci. 31(1):11-22.

Vollrath, L. 1998. The pineal organ. Springer-Verlag Berlin Heidelberg. 665 pp.

Wittkowski, W. 1998. Tanycytes and pituicytes: morphological and functional aspects of neuroglial interaction. Micr Res Tech. 41:29–42.

Ye, W., H. Wang, F. Wang, and J. Wang. 2018. Morphology and ultrastructure of the hypophysis in Bactrian Camels (Camelus bactrianus). Int. J. Morphol. 36(4), 1316-13